

Aggregation and Host–Guest Interactions in Dansyl-Substituted Poly(acrylate)s in the Presence of β -Cyclodextrin and a β -Cyclodextrin Dimer in Aqueous Solution: A UV–Vis, Fluorescence, ^1H NMR, and Rheological Study

Jie Wang,[†] Duc-Truc Pham,[‡] Tak W. Kee,[‡] Scott N. Clifton,[‡] Xuhong Guo,[†] Philip Clements,[‡] Stephen F. Lincoln,^{*,‡} Robert K. Prud'homme,[§] and Christopher J. Easton[⊥]

[†]State Key Laboratory of Chemical Engineering, East China University of Science and Technology, Shanghai, 200237, China

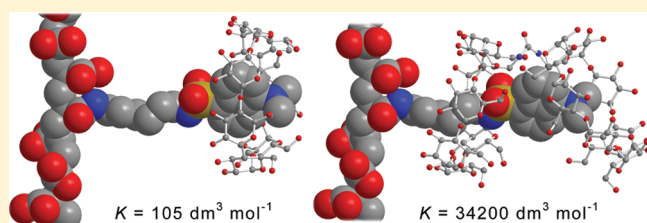
[‡]School of Chemistry and Physics, University of Adelaide, Adelaide, SA 5005, Australia

[§]Department of Chemical Engineering, Princeton University, Princeton, New Jersey 08544, United States

[⊥]Research School of Chemistry, Australian National University, Canberra, ACT 0200, Australia

S Supporting Information

ABSTRACT: A UV–vis, steady-state, and time-resolved fluorescence 2D ^1H NOESY NMR spectroscopic and rheological study of new poly(acrylate)s 3% randomly substituted with either *N*-(2-aminoethyl)-, *N*-(6-aminoethyl)-, or *N*-(12-aminododecyl)-5-dansyl-sulfonamide to give the substituted polymers PAADSen, PAADShn, and PAADSddn, respectively, is reported. Their dansyl substituent aggregation and complexation by β -cyclodextrin, βCD , and its covalently linked dimer *N,N'*-bis(6^A-deoxy-6^A- β -cyclodextrin)urea, $66\beta\text{CD}_2\text{ur}$, is also reported. The βCD complexation of the dansyl substituents is characterized by apparent complexation constants, $K = 89$, 105, and 55 $\text{dm}^3 \text{mol}^{-1}$ for PAADSen, PAADShn, and PAADSddn, respectively, and the analogous complexations by $66\beta\text{CD}_2\text{ur}$ are characterized by $K = 3.04 \times 10^3$, 3.42×10^4 , and $2.42 \times 10^5 \text{ dm}^3 \text{mol}^{-1}$ at pH 7.0 in aqueous 0.10 mol dm^{-3} NaCl at 298.2 K. Under the same conditions the dansyl substituent shows three fluorescence decay constants assigned to the aggregated ($\tau_1 = 2.2$, 2.5, and 3.2 ns), single ($\tau_2 = 5.0$, 5.3, and 9.5 ns), βCD ($\tau_3 = 13.2$, 11.7 ns, and undetected), and $66\beta\text{CD}_2\text{ur}$ complexed dansyl substituent states ($\tau_3 = 13.9$, 20.8, and 19.3 ns) where the values in each data set correspond to PAADSen, PAADShn, and PAADSddn solutions, respectively. 2D ^1H NOESY NMR spectroscopy provides additional insight into dansyl substituent complexation by βCD and $66\beta\text{CD}_2\text{ur}$, as do rheological studies. These data are interpreted in terms of the factors affecting dansyl substituent fluorescence quenching and the impact of tether length on dansyl substituent aggregation, complexation, and network formation.



INTRODUCTION

The use of fluorescent polymers has been reported in studies of scintillators,¹ luminescent solar concentrators,² laser-resistant materials,³ fiber-optic sensors,⁴ and laser dyes.⁵ Such polymers usually consist of a backbone substituted with fluorophores such as the naphthyl,^{6–9} pyrenyl,^{7,10–14} and dansyl^{8,15–19} entities. The fluorescence intensities and lifetimes of such fluorophores are sensitive to local environment such that steady-state and time-dependent fluorescence studies have provided considerable insight into polymer interactions.^{6–19}

As part of an exploration of substituent interactions of randomly substituted poly(acrylate)s, PAA,^{20–25} we report a UV–vis, steady-state, and time-resolved fluorescence and 2D ^1H NOESY NMR study of the variation of dansyl substituent spectroscopic response to environmental change at the molecular level in dilute aqueous solution. These observations are used to interpret macroscopic observations gained through rheological studies of variations in the viscosities in terms of network

formation in more concentrated solutions. The poly(acrylate)s studied are 3% randomly substituted by *N*-(2-aminoethyl)-, *N*-(6-aminoethyl)-, and *N*-(12-aminododecyl)-5-dansylsulfonamide, PAADSen, PAADShn, and PAADSddn, in which the dansyl substituent tether length progressively increases (Scheme 1). This facilitates studies of the effect of tether length on dansyl substituent, aggregation and complexation by β -cyclodextrin, βCD , and the linked dimer *N,N'*-bis(6^A-deoxy-6^A- β -cyclodextrin)urea, $66\beta\text{CD}_2\text{ur}$, in dilute aqueous solution where interactions occur dominantly within individual substituted poly(acrylate) strands.

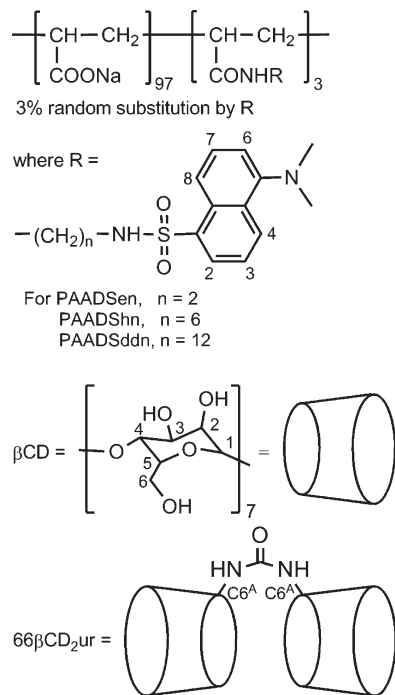
In more concentrated solutions aggregation of dansyl substituents between substituted poly(acrylate) strands occur to form networks which may either be disrupted through βCD forming

Received: September 8, 2011

Revised: November 3, 2011

Published: November 22, 2011

Scheme 1. 3% Randomly Substituted Poly(acrylate)s, β CD, and the 66β CD₂ur Dimer in Which Two β CD Are Each Substituted at the C6^A Carbon of One Glucopyranose Unit by Urea and Covalently Linked^a



^a The narrow and wide ends of the truncated cone representing β CD correspond to the rings of primary and secondary hydroxyl groups, respectively.

host–guest complexes with individual dansyl substituents or may be strengthened through 66β CD₂ur simultaneously complexing dansyl substituents from adjacent substituted poly(acrylate) strands. This study increases understanding of the rapidly expanding field in which cyclodextrin host–guest chemistry is generating a wide variety of aqueous and solid polymer systems and networks.^{20–32}

EXPERIMENTAL SECTION

Materials. 1,2-Diaminoethane, 1,6-diaminohexane, and 1,12-diaminododecane (Strem), dansyl chloride (Fluka), tetrahydrofuran (Ajax), *N*-methylpyrrolidin-2-one (Merck), dicyclohexylcarbodiimide (Aldrich), and β CD (Nihon Shokuhin Kako Co.) were used as supplied. Poly(acrylic acid) ($M_w = 250\,000$, $M_w/M_n \approx 2$) was purchased from Aldrich as a 35 wt % aqueous solution and freeze-dried to a constant weight. Basic alumina (Fluka) was supplied at Brockman activity I, and the appropriate amount of water was added to give Brockman activity III.

Preparation of *N*-(2-Aminoethyl)-5-dansylsulfonamide. A solution of dansyl chloride (270 mg, 1 mmol) in tetrahydrofuran (25 cm³) was added dropwise over 3 h to a vigorously stirred solution of 1,2-diaminoethane (1.0 g, 17 mmol) in tetrahydrofuran (10 cm³). The solvent was removed under reduced pressure, and the residue was dissolved in dichloromethane (20 cm³) and 10% hydrochloric acid (20 cm³). The layers were separated, and the aqueous layer was washed with dichloromethane (3 \times 20 cm³). This aqueous solution was then made basic by addition of 10% w/w aqueous sodium hydroxide and extracted with dichloromethane (5 \times 20 cm³). The dichloromethane

solutions were combined and washed successively with water (5 \times 50 cm³) and brine (50 cm³) and dried over magnesium sulfate. The solution was filtered, and the solvent was removed under reduced pressure to give the crude product as a yellow-green waxy solid. This was recrystallized from benzene/hexane to give the pure products as light green needles (158 mg, 54%). ¹H NMR: δ_H (DMSO-*d*₆) 8.51 (d, 1H, $J = 8.4$ Hz, ArH); 8.35 (d, 1H, $J = 8.7$ Hz, ArH); 8.15 (d, 1H, $J = 8.7$ Hz, ArH); 7.68 (m, 2H, ArH); 7.31 (d, 1H, $J = 7.5$ Hz, ArH); 2.87 (s, 6H, N(CH₃)₂); 2.82 (t, 2H, SO₂NHCH₂); 2.50 (t, 2H, CH₂NH₂). GCMS calcd for C₁₄H₁₉N₃O₂S m/z 293.12; found 293.20.

Preparation of *N*-(6-Aminohexyl)-5-dansylsulfonamide.

A solution of dansyl chloride (270 mg, 1 mmol) in tetrahydrofuran (25 cm³) was added dropwise over 3 h to a vigorously stirred solution of 1,6-diaminohexane (2.0 g, 17 mmol) in tetrahydrofuran (25 cm³). The solvent was removed under reduced pressure, and the residue was dissolved in dichloromethane (20 cm³) and 10% hydrochloric acid (20 cm³). The layers were separated, and the aqueous layer was washed with dichloromethane (3 \times 20 cm³). This aqueous solution was made basic by addition of 10% w/w aqueous sodium hydroxide and extracted with dichloromethane (5 \times 20 cm³). The dichloromethane solutions were combined and washed successively with water (5 \times 50 cm³) and brine (50 cm³) and dried over magnesium sulfate. The solvent was removed under reduced pressure to give a yellow-green oil. This was dissolved in dichloromethane (5 cm³) and loaded onto basic alumina column (160 \times 15 mm, Brockman activity III) which was eluted with a gradient of dichloromethane:methanol from 100:0 to 80:20. Fractions containing the product were combined and concentrated under reduced pressure to give the product as a light green oil (180 mg, 52%). ¹H NMR: δ_H (DMSO-*d*₆) 8.51 (d, 1H, $J = 9.0$ Hz, ArH); 8.35 (d, 1H, $J = 8.7$ Hz, ArH); 8.14 (d, 1H, $J = 6.3$ Hz, ArH); 7.68 (m, 2H, ArH); 7.31 (d, 1H, $J = 7.2$ Hz, ArH); 2.86 (s, 6H, N(CH₃)₂); 2.82 (t, 2H, SO₂NHCH₂); 2.43 (t, 2H, CH₂NH₂). GCMS calcd for C₁₈H₂₇N₃O₂S m/z 349.18; found 349.20.

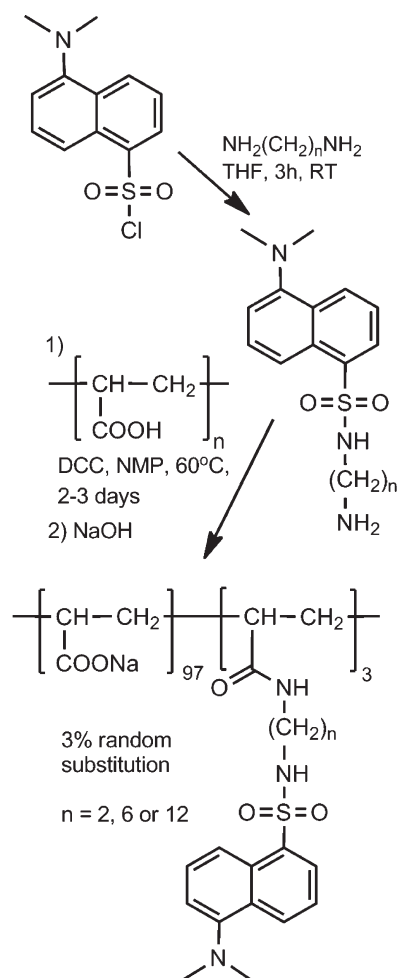
Preparation of *N*-(12-Aminododecyl)-5-dansylsulfonamide.

A solution of dansyl chloride (270 mg, 1 mmol) in tetrahydrofuran (25 cm³) was added dropwise over 3 h to a vigorously stirred solution of 1,12-diaminododecane (2.0 g, 10 mmol) in tetrahydrofuran (25 cm³). After stirring overnight the yellow-green reaction mixture was filtered. The solvent was removed under reduced pressure, and the residue was dissolved in dichloromethane (20 cm³). This solution was washed successively with 10% w/w aqueous sodium hydroxide (3 \times 30 cm³), water (5 \times 50 cm³), and brine (50 cm³) and dried over magnesium sulfate. The filtered solution was evaporated under reduced pressure to give a white solid. This was suspended in dichloromethane (10 cm³), filtered, and loaded onto a basic alumina column (160 \times 15 mm, Brockman activity III). The column was eluted with a gradient of dichloromethane:methanol from 100:0 to 90:10. Fractions containing the product were combined and concentrated under reduced pressure to give the product as a light green oily solid (265 mg, 61%). ¹H NMR: δ_H (DMSO-*d*₆) 8.50 (d, 1H, $J = 8.4$ Hz, ArH); 8.34 (d, 1H, $J = 8.4$ Hz, ArH); 8.14 (d, 1H, $J = 7.2$ Hz, ArH); 7.67 (m, 2H, ArH); 7.29 (d, 1H, $J = 7.5$ Hz, ArH); 2.86 (s, 6H, N(CH₃)₂); 2.82 (t, 2H, SO₂NHCH₂); 2.52 (t, 2H, CH₂NH₂). GCMS calcd for C₂₄H₃₉N₃O₂S m/z 433.28; found 433.45.

Preparation of 3% Substituted Poly(acrylate)s. The new PAADSen, PAADShn, and PAADSddn 3% randomly substituted poly(acrylate)s were prepared from poly(acrylic acid) and the respective aliphatic amine substituted dansylsulfonamide in the presence of dicyclohexylcarbodiimide in *N*-methyl-2-pyrrolidone at 60 °C in a similar manner to that reported for other substitutions² and according to the general procedure shown in Scheme 2.^{20,21,24,25} The three substituted poly(acrylate)s were isolated as the sodium salts. Yield: 70–80%.

Characterization. Routine ¹H NMR spectra were recorded on a Varian Gemini ACP-300 spectrometer operating at 300.145 MHz. The degrees of substitution of the carboxyl groups in poly(acrylate) (PAA) in

Scheme 2. General Scheme for the Preparation of 3% Randomly Substituted Poly(acrylate)s



PAADSen, PAADShn, and PAADSddn were determined to be 3.0% by ^1H NMR spectroscopy through a comparison of the relative resonance areas of the dansyl H2–4,6–8 and methyl protons and PAA methylene protons. The 2D ^1H NOESY NMR spectra were recorded on a Varian Inova 600 spectrometer operating at 599.957 MHz using a standard pulse sequence with a mixing time of 0.3 s. Solutions for host–guest complexation studies contained either PAADSen, PAADShn, or PAADSddn (10 mg) and βCD (3.5 mg) in 1 cm^3 D_2O such that the βCD and dansyl substituents of the substituted poly(acrylate)s were equimolar. The pD was adjusted to 7.0 ± 0.2 with 0.10 mol dm^{-3} NaOD in D_2O for each solution, which was also 0.10 mol dm^{-3} in NaCl. Solutions were allowed to equilibrate at the thermostated probe temperature of $298.2 \pm 0.1\text{ K}$ for 30 min in 5 mm NMR tubes prior to recording their spectra.

The UV–vis and fluorescence spectra of solutions 0.10 mol dm^{-3} in NaCl whose pH was adjusted to 7.0 ± 0.2 with 0.10 mol dm^{-3} NaOH were recorded with a Varian-Cary 300 UV–vis spectrophotometer using 1 cm path length matched quartz cells and a Varian-Cary Eclipse fluorimeter using standard cuvettes, respectively. The fluorescence excitation wavelength was 331 nm in all cases, and excitation and emission slit widths were set at 5 nm. Solutions were thermostated to within $\pm 0.1\text{ K}$ of the desired temperature.

The model used for determining the apparent complexation constant assumes that the dansyl groups in PAADSen, PAADShn, and PAADSddn exist in aggregated and monomeric forms in a labile

equilibrium which continually readjusts as the monomer form is complexed by either βCD or $66\beta\text{CD}_{2\text{ur}}$ to form the 1:1 host–guest complexes exemplified by $\beta\text{CD}.\text{PAADSen}$ and $66\beta\text{CD}_{2\text{ur}}.\text{PAADSen}$. Thus, βCD complexes PAADSen according to eq 1.



The apparent complexation constant, K , at equilibrium is given by

$$K = [\beta\text{CD}.\text{PAADSen}] / [\beta\text{CD}][\text{PAADSen}] \quad (2)$$

Given that $[\text{PAADSen}]_{\text{total}}$ and $[\beta\text{CD}]_{\text{total}}$ are the initial concentrations of the two complexation partners

$$[\text{PAADSen}]_{\text{total}} = [\beta\text{CD}.\text{PAADSen}] + [\text{PAADSen}] \quad (3)$$

$$[\beta\text{CD}]_{\text{total}} = [\beta\text{CD}.\text{PAADSen}] + [\beta\text{CD}] \quad (4)$$

the fluorescence at a particular wavelength is given by

$$F = I_{\text{PAADSen}}[\text{PAADSen}] + I_{\beta\text{CD}.\text{PAADSen}}[\beta\text{CD}.\text{PAADSen}] \quad (5)$$

where F , I_{PAADSen} , and $I_{\beta\text{CD}.\text{PAADSen}}$ represent the observed fluorescence and apparent molar fluorescences of PAADSen and $\beta\text{CD}.\text{PAADSen}$, respectively. Fluorescence measurements were made in 1 cm path length cuvettes over the range 450–600 at 0.5 nm intervals as the βCD concentration was varied. The value of K was determined by best fitting the variation of the fluorescence spectra in the range 450–600 at 0.5 nm intervals to an algorithm based on eqs 2–5 as the βCD concentration was varied using the HypSpec protocol.³³ The same protocol was used for the other βCD systems and the $66\beta\text{CD}_{2\text{ur}}$ systems. Algorithms for complexations involving 1:2 and 2:1 host/guest stoichiometries in addition to, or separate from, 1:1 stoichiometry could not be fitted to the data.

Time-Resolved Fluorescence Measurements. Time-resolved fluorescence measurements were made on 1.0 wt % substituted poly(acrylate) solutions where the total dansyl substituent concentration was $2.95 \times 10^{-3}\text{ mol dm}^{-3}$ in aqueous 0.10 mol dm^{-3} NaCl at pH 7.0 and 298.2 K using the time-correlated single photon counting (TCSPC) technique.³⁴ The laser source was a mode-locked Ti-sapphire laser (Spectra Physics Tsunami), tunable from 720 to 1000 nm with a repetition rate of 80 MHz. The fundamental output from the Ti-sapphire oscillator was modulated by a Pockels cell (Model 350-160, Conoptics Inc.) to reduce the repetition rate to about 16 MHz and was subsequently frequency doubled by focusing tightly into a 0.5 mm BBO crystal (Eksma Optics). The resulting blue light, which had a central wavelength of 400 nm, provided the excitation source. A half-wave plate before a vertical polarizer ensured the polarization of the excitation light. The fluorescence decays were collected using a time-resolved fluorescence spectrometer (Ultrafast System Halcyone). Emission at 540 nm was collected through a double monochromator fitted with a slit with a 1 nm band-pass. The instrument response function of the apparatus had a full width at half-maximum (fwhm) of 1 ns. The acquisition time window had a width of 62.5 ns with 0.05 ns time steps. A cuvette of 0.2 cm path length was used for the time-resolved measurements of the samples. Multiexponential fits of the time-resolved fluorescence traces were obtained using the Ultrafast System Surface Explorer protocol.³⁵

Rheology. Rheological measurements were carried out with a Physica MCR 501 (Anton Parr GmbH) stress-controlled rheometer with a 25 mm cone and plate geometry. Temperature was controlled at $298.2 \pm 0.1\text{ K}$ by a Peltier plate. All studies were carried out in 0.10 mol dm^{-3} aqueous NaCl solution at pH 7.0 adjusted with 0.10 mol dm^{-3} aqueous NaOH solution.

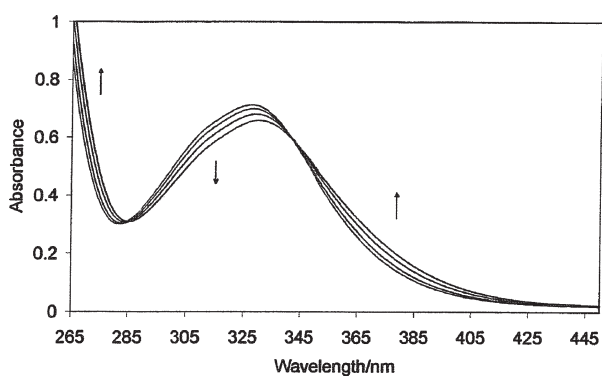


Figure 1. UV-vis absorption spectra of PAADSen where the dansyl substituent concentration is $1.5 \times 10^{-4} \text{ mol dm}^{-3}$ at 283.2, 303.2, 323.2, and 343.2 K in aqueous 0.01 mol dm^{-3} NaCl at pH 7.0. The arrows indicate the direction of change with increase in temperature. Isosbestic points occur at 284 and 342 nm, and λ_{max} and the molar absorbance, ϵ_{max} , respectively change from 327 nm and $4752 \text{ dm}^3 \text{ mol}^{-1} \text{ cm}^{-1}$ at 283.2 K to 329 nm and $4392 \text{ dm}^3 \text{ mol}^{-1} \text{ cm}^{-1}$ at 343.2 K. The path length is 1 cm.

RESULTS AND DISCUSSION

Preparation of 3% Randomly Dansyl-Substituted Poly(acrylate)s. The new randomly substituted dansyl-substituted poly(acrylate)s were prepared with differing length linear aliphatic tethers as shown in Scheme 2. The tethers were attached to the dansylsulfonamide by reacting with the appropriate linear aliphatic diamine at room temperature in tetrahydrofuran (THF) for 3 h. These amine-substituted dansylsulfonamide were then reacted with poly(acrylic acid) of $M_w = 250\,000$ and $M_w/M_n \approx 2$ in *N*-methyl-2-pyrrolidone (NMP) in the presence of dicyclohexylcarbodiimide (DCC) at 60°C for 2–3 days in a similar manner to that reported elsewhere for other substitutions.^{20,21,24,25} The reacted solutions were made basic with NaOH, and the sodium poly(acrylate)s were separated and purified by dialysis.

UV-Vis Studies of Dansyl-Substituted Poly(acrylate)s. The dansyl substituent UV-vis spectra of either 3% randomly substituted PAADSen (Figure 1), PAADShn, or PAADSddn in 0.10 mol dm^{-3} NaCl aqueous solution at pH 7.0 exhibit reversible temperature variations and are characterized by two isosbestic points. This indicates that the dansyl substituents experience two dominant environments whose populations are temperature dependent and which are considered to be the single and aggregated states within a single substituted poly(acrylate) strand. (In these solutions where the poly(acrylate) is 0.05 wt % and the dansyl substituent total concentration is $1.5 \times 10^{-4} \text{ mol dm}^{-3}$, interaction between poly(acrylate) strands is likely to be minimal.²¹) In the absence of the individual single and aggregated dansyl substituent spectra, this intramolecular equilibrium cannot be quantified. However, as temperature increases, λ_{max} increases and ϵ_{max} decreases which, on the assumption that dansyl substituent aggregation decreases with increase in temperature, is consistent with λ_{max} and ϵ_{max} for single dansyl substituents being larger and smaller, respectively, than those of the dansyl substituent aggregate. At 283.2 K the dansyl λ_{max} (nm) are similar, and the molar absorbance ϵ_{max} ($\text{dm}^3 \text{ mol}^{-1} \text{ cm}^{-1}$) decreases in the sequence PAADSen (327 and 4752), PAADShn (327 and 4198), PAADSddn (328 and 3571), as shown by the first and second values in parentheses.

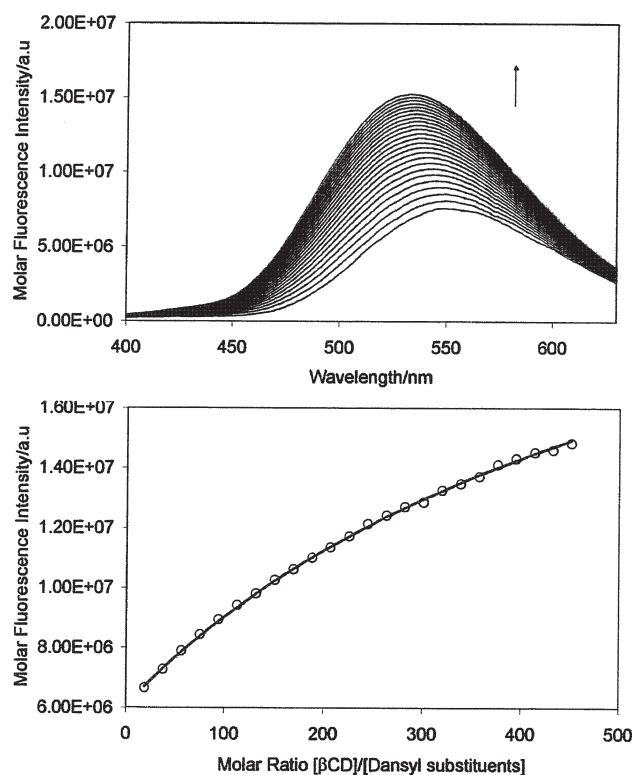


Figure 2. (top) Fluorescence increase of a PAADShn solution for which the dansyl substituent concentration is $1.0 \times 10^{-5} \text{ mol dm}^{-3}$ (corresponding to 0.0034 wt % in PAADShn) with 25 sequential additions (25 mm^3 each) of βCD solution ($1.41 \times 10^{-2} \text{ mol dm}^{-3}$). Both aqueous solutions are 0.10 mol dm^{-3} in NaCl with a pH = 7.0 at 298.2 K. The arrow indicates the increase in fluorescence with each addition of βCD solution. Excitation is at 331 nm. (bottom) Fluorescence variation at 524 nm and the line representing the best fit of an algorithm for a 1:1 host-guest complexation by βCD of a dansyl substituent to data at 0.5 nm intervals over the wavelength range 450–600 nm.

When the total dansyl substituent concentrations are increased in the range 5.64×10^{-6} – $1.41 \times 10^{-3} \text{ mol dm}^{-3}$ in solutions of either PAADSen, PAADShn, or PAADSddn in 0.10 mol dm^{-3} NaCl aqueous solution at pH 7.0 and 298.2 K solutions, the absorbance of the dansyl substituent increases linearly over most of the range and shows a systematic small negative deviation from linearity at the higher end of the concentration range consistent with intermolecular interactions between dansyl substituents on different poly(acrylate) strands occurring. However, these small departures from linearity are insufficient to quantitatively characterize this interaction. The highest concentration studied corresponds to a 0.5 wt % substituted poly(acrylate) solution where the shared solution volumes of the three substituted poly(acrylate)s are small, and consequently any inter-poly(acrylate) strand dansyl-dansyl substituent interaction is likely to be minor.²¹ While these data can only be interpreted qualitatively, time-dependent fluorescence studies allow single and aggregated dansyl substituent excited state lifetimes to be quantified as is discussed below.

Fluorescence and UV-Vis Studies of Dansyl Substituent Complexation by βCD and $66\beta\text{CD}_2\text{ur}$. The variation of the fluorescence of the dansyl substituent of PAADShn with increasing βCD concentration (Figure 2) is consistent with the formation of a dominant 1:1 βCD :dansyl substituent host-guest

Table 1. Fluorescence Titration and 2D ^1H NOESY NMR Data

system	fluorescence data			2D ^1H NMR NOESY data βCD or $66\beta\text{CD}_2\text{ur}$ cross-peaks	
	λ_{max} (nm)	I_{max} (au)	K ($\text{dm}^3 \text{mol}^{-1}$)	with dansyl substituent	with tether to substituent
dansyl substituent					
PAADSen	556	68			
PAADShn	550	76			
PAADSddn	546	103			
complexed dansyl substituent					
PAADSen/ βCD	524	378	89 ± 5	moderate	none
PAADShn/ βCD	524	406	105 ± 5	moderate	weak
PAADSddn/ βCD	542	121	55 ± 3	moderate	strong
PAADSen/ $66\beta\text{CD}_2\text{ur}$	524	199	3040 ± 100	moderate	none
PAADShn/ $66\beta\text{CD}_2\text{ur}$	506	618	34200 ± 500	strong	weak
PAADSddn/ $66\beta\text{CD}_2\text{ur}$	513	681	242000 ± 5000	strong	strong

complex characterized by an apparent complexation constant, $K = 105 \text{ dm}^3 \text{mol}^{-1}$ with $\lambda_{\text{max}} = 524 \text{ nm}$ and $I_{\text{max}} = 406 \text{ au}$ for the βCD complexed dansyl substituent. Similar variations in fluorescence occur for PAADSen and PAADSddn for which $K = 89$ and $55 \text{ dm}^3 \text{mol}^{-1}$, respectively (Table 1). Thus, K varies within a factor of 2, and the change in environment of the dansyl substituent upon complexation by βCD is reflected by a decrease in λ_{max} and an increase in I_{max} of the complexed dansyl substituents by comparison with that of the uncomplexed dansyl substituents of PAADSen and PAADShn (Table 1). This is consistent with a change from an aqueous environment to the hydrophobic environment of the βCD annular interior. The decrease in λ_{max} and increase in I_{max} for the PAADSddn system are comparatively much smaller consistent with the occurrence of a lesser dansyl substituent environmental change occurring upon complexation. This is probably because a substantial proportion of the βCD passes over the dansyl substituent to complex the dodecyl tether while the remainder of the βCD complexes the dansyl substituent as is indicated by the ^1H NMR studies discussed below.

Complexation of the dansyl substituents of PAADSen, PAADShn, and PAADSddn by $66\beta\text{CD}_2\text{ur}$ is much stronger than complexation by βCD (Table 1). This is exemplified by the variation of the fluorescence of the dansyl substituent of PAADShn with increasing concentration of $66\beta\text{CD}_2\text{ur}$ (Figure 3), consistent with the formation of a dominant 1:1 $66\beta\text{CD}_2\text{ur}$:dansyl substituent host–guest complex characterized by an apparent complexation constant, $K = 34200 \text{ dm}^3 \text{mol}^{-1}$ with $\lambda_{\text{max}} = 506 \text{ nm}$ and $I_{\text{max}} = 619 \text{ au}$ for the complexed dansyl substituent. Similar variations in fluorescence occur for the PAADSen and PAADSddn systems for which $K = 3040$ and $242000 \text{ dm}^3 \text{mol}^{-1}$, respectively (Table 1). Thus, K increases 80-fold consistent with increasing cooperativity in binding of the dansyl substituent and its tether in both cyclodextrin annuli of $66\beta\text{CD}_2\text{ur}$ as tether length increases and steric hindrance caused by the poly(acrylate) backbone lessens. This also causes substantial decreases in λ_{max} and increases in I_{max} of the complexed dansyl substituent by comparison with that of the uncomplexed dansyl substituent. However, the change in λ_{max} and I_{max} for the PAADSen system is much less than for the PAADShn and PAADSddn systems probably because steric hindrance from the poly(acrylate) backbone causes the complexation of the dansyl substituent of PAADSen to be largely limited to a single

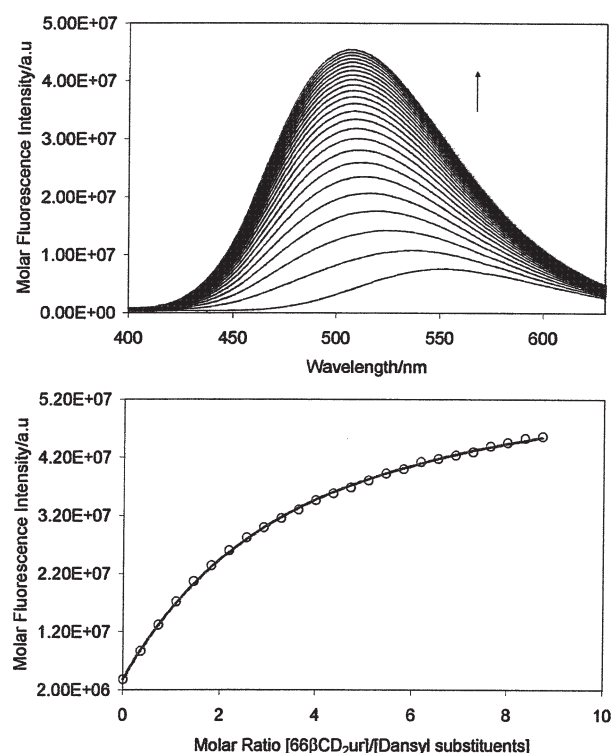


Figure 3. (top) Fluorescence increase of a PAADShn solution for which the dansyl substituent concentration is $1.0 \times 10^{-5} \text{ mol dm}^{-3}$ (corresponding to 0.0034 wt % in PAADShn) with 25 sequential additions (6.5 mm^3 each) of $66\beta\text{CD}_2\text{ur}$ solution ($1.09 \times 10^{-3} \text{ mol dm}^{-3}$). Both aqueous solutions are 0.10 mol dm^{-3} in NaCl at pH 7.0 at 298.2 K. The arrow indicates the increase in fluorescence with each addition of βCD solution. Excitation is at 331 nm. (bottom) Fluorescence variation at 506 nm and the line representing the best fit of an algorithm for a 1:1 host–guest complexation by $66\beta\text{CD}_2\text{ur}$ of a dansyl substituent to data at 0.5 nm intervals over the wavelength range 450–600 nm.

cyclodextrin annulus of $66\beta\text{CD}_2\text{ur}$ such that it experiences a smaller environmental change than is the case in the analogous PAADShn and PAADSddn systems.

The UV–vis spectrum of a PAADShn solution where the dansyl substituent concentration is $1.5 \times 10^{-4} \text{ mol dm}^{-3}$ also

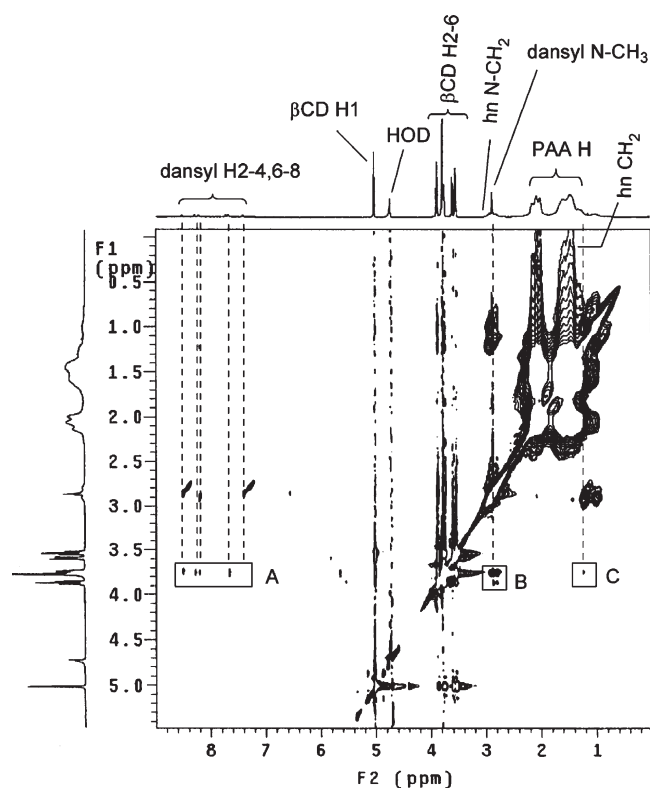
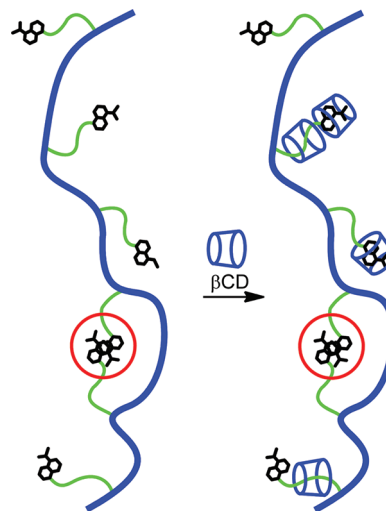


Figure 4. 2D ^1H NOESY NMR 600 MHz spectrum of a D_2O solution in which the PAADShn dansyl substituent and βCD concentrations are $2.95 \times 10^{-3} \text{ mol dm}^{-3}$ (PAADShn concentration is 1.0 wt %) at pD 7.0. The rectangles A, B, and C enclose the cross-peaks arising from interaction of the βCD annular H3, H5, and H6 protons with dansyl substituent H2–4,6–8, dansyl substituent methyl (N– CH_3), and hexyl tether (hn CH_2) protons.

shows a systematic increase in λ_{max} with isosbestic points occurring at 295 and 331 nm with increase in βCD concentration under the same conditions as for the analogous fluorescence studies. This is consistent with the formation of a dominant 1:1 βCD :dansyl substituent host–guest complex and an increase in λ_{max} of the complexed dansyl substituent. However, the magnitude of the absorbance variation is insufficient for quantitative characterization of the βCD :dansyl substituent host–guest complex. Analogous changes in UV–vis spectra occur in the PAADSen and PAADSddn systems.

2D ^1H NOESY NMR Studies of Dansyl Substituent Complexation by βCD and $66\beta\text{CD}_2\text{ur}$. The 2D NOESY ^1H NMR spectrum of a D_2O solution of PAADShn equimolar in βCD and dansyl substituents shows moderate cross-peaks arising from interaction between the βCD annular H3,5,6 protons and the dansyl H2–4,6–8 aromatic and methyl protons and the hexyl tether protons (Figure 4). (Cross-peak intensity is assessed by comparison with that of cross-peaks arising from interaction between the dansyl substituent aromatic protons and methyl protons in the same spectrum.) This is consistent with both the hexyl tether and the dansyl substituent complexing within the βCD annulus. While cross-peaks arise from interaction between the βCD annular H3,5,6 protons and the dansyl H2–4,6–8 and methyl protons for the analogous spectra of the PAADSen and PAADSddn solutions occur, no cross-peaks occur for the ethyl tether protons of PAADSen whereas strong cross-peaks occur for the dodecyl tether protons of the PAADSddn (Table 1).

Scheme 3. Interactions in a PAADSddn Strand Showing Two Possible Modes of Complexation of Dansyl Substituents by βCD , One Double Complexation Mode, and the Single and Aggregated (Ringed in Red and Shown for Simplicity As Dimers Formed by Adjacent Dansyl Substituents) Forms of the Dansyl Substituents^a



^a The thick blue line represents the poly(acrylate) backbone, the shorter green lines represent the dodecyl tethers, and the truncated cones represent βCD .

For protons at similar interaction distances, the strength of a cross-peak is proportional to the number of protons involved and the dodecyl tether is therefore expected to produce the strongest cross-peaks when complexed in the βCD annulus. Nevertheless, the absence of any cross-peaks associated with the ethyl tether suggests a variation of host–guest complexation with tether length. Thus, the long dodecyl tether of PAADSddn complexes in the βCD annulus, as do octadecyl substituents on other substituted poly(acrylate)s,²¹ and competes with the dansyl substituent for occupancy of the βCD annulus as was inferred earlier from the fluorescence studies. For PAADSen and PAADShn the shorter tethers render this competition less effective.

Collectively, the temperature-dependent UV–vis, fluorescence, and 2D ^1H NOESY NMR spectroscopic data suggest that the dansyl substituent and the dodecyl tether of PAADSddn are complexed by βCD singly as shown in Scheme 3 together with single and aggregated dodecyl substituents. The βCD competitive complexation results in a lesser proportion of the dansyl substituents occupying the βCD annulus upon complexation such that the fluorescence decrease in λ_{max} and the increase in I_{max} for the PAADSddn system are less than for the PAADSen and PAADShn systems. (It is possible that a dansyl substituent and its dodecyl tether could be complexed by two βCD s as is also shown in Scheme 3, but such complexation cannot be distinguished from the two singly βCD complexed forms on the basis of the experimental data.)

The 2D NOESY ^1H NMR spectrum of a D_2O solution of PAADSddn equimolar in $66\beta\text{CD}_2\text{ur}$ and dansyl substituents shows strong cross-peaks arising from interaction between the $66\beta\text{CD}_2\text{ur}$ annular H3,5,6 protons, the dansyl H2–4,6–8 aromatic and methyl protons, and the dodecyl tether protons (Figure 5). This indicates that both the dansyl substituent and

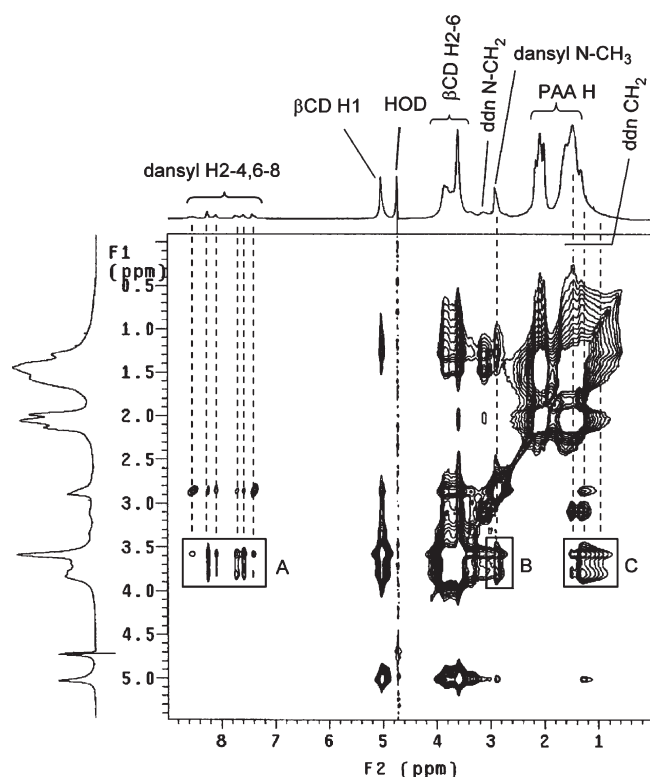


Figure 5. 2D ^1H NOESY NMR 600 MHz spectrum of a D_2O solution in which the dansyl substituent and $66\beta\text{CD}_2\text{ur}$ concentrations are $2.95 \times 10^{-3} \text{ mol dm}^{-3}$ in 3% substituted PAADSddn and $66\beta\text{CD}_2\text{ur}$ (PAADSddn concentration is 1.0 wt %) at pD 7.0. The rectangles A, B, and C enclose the cross-peaks arising from interaction of the $66\beta\text{CD}_2\text{ur}$ annular H3, H5, H6 protons with the dansyl H2–4,6–8 protons, dansyl (N– CH_3), and dodecyl tether (ddn CH_2) protons.

the dodecyl tether complex within the cyclodextrin annuli of $66\beta\text{CD}_2\text{ur}$. While the 2D NOESY ^1H NMR spectrum of the $66\beta\text{CD}_2\text{ur}$ /PAADS_{en} solution also shows cross-peaks arising from interaction of the $66\beta\text{CD}_2\text{ur}$ annular H3, H5, H6 protons with the dansyl H2–4,6–8 and methyl protons, no cross-peaks are observed for the ethyl tether protons. As for the analogous βCD solution, this is consistent with the length of the ethyl tether being insufficient to allow its complexation by $66\beta\text{CD}_2\text{ur}$ because of steric hindrance arising from the poly(acrylate) backbone. The 2D NOESY ^1H NMR spectrum of the $66\beta\text{CD}_2\text{ur}$ /PAADS_{hn} solution shows moderate cross-peaks arising from interaction of the $66\beta\text{CD}_2\text{ur}$ annular H3, H5, H6 protons with the dansyl H2–4,6–8 and methyl protons and also weak cross-peaks arising from a similar interaction with the hexyl protons, consistent with the increased tether length decreasing the effect of steric interactions on complexation. The overall effect of tether length on $66\beta\text{CD}_2\text{ur}$ complexation is illustrated by the energy-minimized structures in Figure 6 obtained using the Chem3D MM2 protocol.³⁶

In addition to these 1:1 complexations, it is possible that some $66\beta\text{CD}_2\text{ur}$ may also simultaneously complex two dansyl substituents in a single strand of PAADS_{en}, PAADS_{hn}, and PAADS_{ddn}, particularly in the latter case where the longer tether confers greater flexibility. While such simultaneous complexation cannot be distinguished from 1:1 complexation through the fluorescence and ^1H NMR data, the possibility of its occurrence is inferred from the viscosity variations of more concentrated 5.0 wt %

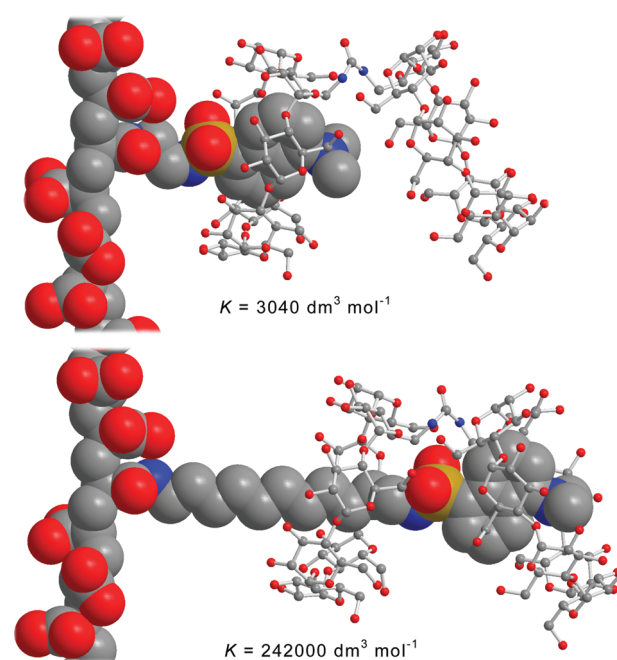


Figure 6. Chem3D MM2 energy-minimized models of the 1:1 $66\beta\text{CD}_2\text{ur}$ host–guest complexes of the dansyl substituent with an ethyl tether (top) and a dodecyl tether (bottom) with their respective complexation constants.

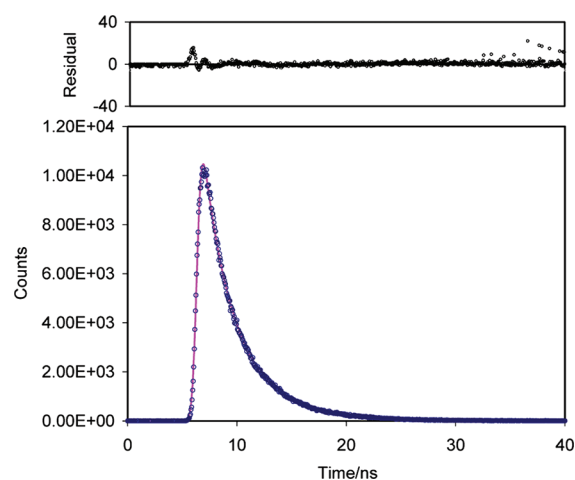


Figure 7. Time-dependent fluorescence at 540 nm of a 1.0 wt % aqueous solution of PAADS_{hn} in which the total dansyl substituent concentration is $2.95 \times 10^{-3} \text{ mol dm}^{-3}$, $[\text{NaCl}] = 0.10 \text{ mol dm}^{-3}$, pH = 7.0 at 298.2 K. The solid line represents the best fit of the data to an algorithm for the fluorescence biexponential decay $A_1 \exp(-t/\tau_1) + A_2 \exp(-t/\tau_2)$, where A_1 and A_2 are the amplitudes of the decay components and τ_1 and τ_2 are the corresponding decay time constants. The resolution is 1 ns.

solutions where the viscosity increases caused by the addition of $66\beta\text{CD}_2\text{ur}$ are attributed to the simultaneous complexation of two dansyl substituents on adjacent PAADS_{en}, PAADS_{hn}, or PAADS_{ddn} strands as is discussed below.

Time-Resolved Fluorescence Studies of Dansyl Substituent Aggregation and Complexation by βCD and $66\beta\text{CD}_2\text{ur}$. Aqueous solutions of PAADS_{en}, PAADS_{hn}, and PAADS_{ddn}

Table 2. Time-Dependent Fluorescence Data^a

system PAADSen	A ₁	τ ₁ (ns)	A ₂	τ ₂ (ns)	A ₃	τ ₃ (ns)
—	0.814	2.2 ± 0.4	0.186	5.0 ± 0.7		
βCD	0.619	2.2	0.187	5.0	0.193	13.2 ± 2.0
βCD ₂ ur	0.470	2.2	0.144	5.0	0.386	13.9 ± 2.1
system PAADShn	A ₁	τ ₁ (ns)	A ₂	τ ₂ (ns)	A ₃	τ ₃ (ns)
—	0.792	2.5 ± 0.4	0.208	5.3 ± 0.7		
βCD	0.532	2.5	0.139	5.3	0.329	11.7 ± 1.8
βCD ₂ ur	0.066	2.5	0.182	5.3	0.709	20.8 ± 3.0
system PAADSddn	A ₁	τ ₁ (ns)	A ₂	τ ₂ (ns)	A ₃	τ ₃ (ns)
—	0.722	3.2 ± 0.5	0.278	9.5 ± 1.4		
βCD	0.618	3.2	0.378	9.5		
βCD ₂ ur	0.175	3.2	0.167	9.5	0.627	19.3 ± 2.9

^a The overall fitting error for τ₁, τ₂, and τ₃ is ±15%.

show a biexponential decay of fluorescence as exemplified by PAADShn in Figure 7. The time-dependent fluorescence intensity time dependence, $I(t)$, is fitted to eq 6:

$$I(t) = A_1 \exp(-t/\tau_1) + A_2 \exp(-t/\tau_2) \quad (6)$$

where A_1 and A_2 are the amplitudes of the decay components assigned to the excited state aggregated and single dansyl substituents, respectively, and τ_1 and τ_2 are the corresponding time constants for the fluorescence decays for all three systems as shown in Table 2. The assignment of τ_1 is made on the basis that it is expected that π - π and other interactions where π - π stacking is stereochemically prevented between dansyl substituents in the excited state aggregates should shorten fluorescence decay time constants, as has been extensively shown for pyrene substituents in other polymer systems.^{11–13} The τ_2 for the excited state single dansyl substituents of PAADSen and PAADShn are similar, but that for PAADSddn is twice as long possibly reflecting the greater length of the dodecyl tether, allowing greater freedom of motion and a shorter spatial residence time and thereby a less effective fluorescence quenching and a longer τ_2 .

In the presence of βCD, fluorescence time dependence for the PAADSen and PAADShn systems becomes triexponential:

$$I(t) = A_1 \exp(-t/\tau_1) + A_2 \exp(-t/\tau_2) + A_3 \exp(-t/\tau_3) \quad (7)$$

where the $A_3 \exp(-t/\tau_3)$ term in eq 7 arises from the βCD.dansyl and 66βCD₂ur.dansyl excited state host–guest complexes. The parameters in Table 2 are derived by fitting the data to eq 7, with the previously derived τ_1 and τ_2 as fixed parameters, to the fluorescence time dependencies. The overall fitting error is ±15%.

The 2-fold increase in τ_3 for the βCD complexed excited state dansyl substituents of PAADSen and PAADShn complexes by comparison with the analogous τ_2 is attributed to a change for the dansyl substituent from the aqueous environment to the hydrophobic βCD annular environment where quenching is less effective. (This interpretation is similar to that made where dansyl substituents are directly tethered to βCD and exist in an equilibrium between the dansyl substituent inside and outside the annulus.^{37–39}) The amplitude of the third fluorescence decay component for PAADSddn is too small for a reliable determination of τ_3 . This is consistent with βCD complexing PAADSddn

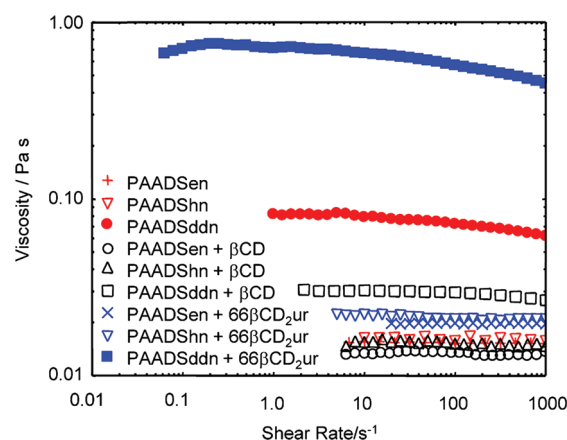


Figure 8. Viscosity shear rate dependence for 5 wt % aqueous 0.10 mol dm⁻³ NaCl solutions at pH 7.0 and 298.2 K of PAADSen, PAADShn, and PAADSddn and their binary mixtures with βCD and 66βCD₂ur in which the mole ratio of the dansyl substituents to either βCD or 66βCD₂ur is unity.

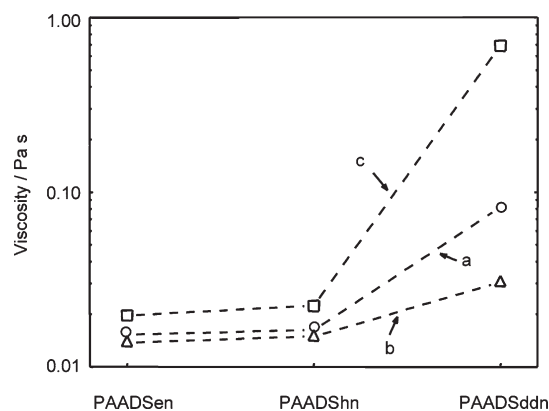
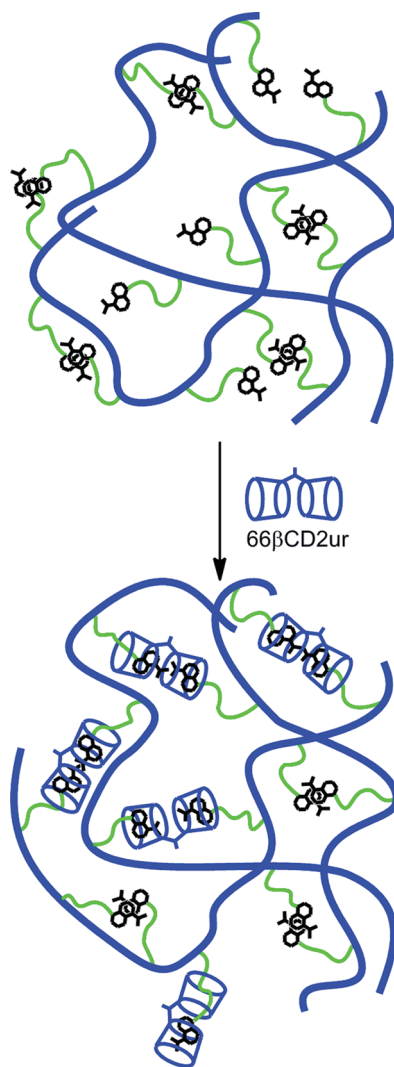


Figure 9. Zero-shear viscosities of 5 wt % aqueous solutions (0.10 mol dm⁻³ NaCl, pH 7.0, 298.2 K) of (a) PAADSen, PAADShn, and PAADSddn and their binary mixtures with (b) native βCD and (c) 66βCD₂ur in which the mole ratio of the dansyl substituents to either βCD or 66βCD₂ur is unity. The individual zero-shear viscosities (Pa·s) are PAADSen (0.015), PAADShn (0.016), PAADSddn (0.081), PAADSen + βCD (0.014), PAADShn + βCD (0.015), PAADSddn + βCD (0.031), PAADSen + 66βCD₂ur (0.020), PAADShn + 66βCD₂ur (0.022), and PAADSddn 66βCD₂ur (0.69).

dominantly with βCD positioned over the long dodecyl tether which has little effect on the dansyl environment or fluorescence and a second form where βCD is positioned over the dansyl entity and enhances fluorescence (Scheme 3). In contrast, the relative shortness of the ethyl and hexyl tethers causes the βCD.PAADSen and βCD.PAADShn complexes to exist dominantly in this second form.

Triexponential dansyl substituent fluorescence time dependences according to eq 7 are also observed in the presence of 66βCD₂ur, and the derived τ_3 appear in Table 2. The similarity of τ_3 for the 66βCD₂ur/PAADSen and βCD/PAADSen systems suggests that the excited state dansyl substituent environments are quite similar despite the 30-fold greater stability of the 66βCD₂ur.PAADSen ground state complex by comparison with that of the βCD.PAADSen complex (Table 1). The τ_3 for the excited states species derived from the more stable 66βCD₂ur.PAADShn and

Scheme 4. (top) Interactions within a 5 wt % PAADSddn Aqueous Solution Showing Inter- and Intrastrand Dansyl Substituent Interactions as Dimerizations although Higher Aggregations May Occur; (bottom) Interactions within a 5 wt % PAADSddn Aqueous Solution after Addition of $66\beta\text{CD}_2\text{ur}$ Showing Dual Host–Guest Interactions between the Cyclodextrin Annuli and the Dansyl Substituents Forming Interstrand Linkages (Some Intrastrand Complexation of Dansyl Substituents May Also Occur) and Inter- and Intrastrand Dansyl Substituent Interactions^a



^a The thick blue line represents the poly(acrylate) backbone, the shorter green lines represent the dodecyl tethers, and the linked truncated cones represent $66\beta\text{CD}_2\text{ur}$.

$66\beta\text{CD}_2\text{ur}$.PAADSddn complexes are longer than those for the excited state of the $66\beta\text{CD}_2\text{ur}$.PAADSen complex, consistent with their longer hexyl and dodecyl tethers allowing greater cooperative in complexation of the dansyl entity by $66\beta\text{CD}_2\text{ur}$ and a greater environmental change and less effective fluorescence quenching. Overall, these time-dependent observations are consistent with the deductions made from the previously discussed steady state UV–vis, fluorescence, and ^1H NMR studies.

Unfortunately, the apparent formation constant for the dansyl substituent aggregation cannot be quantified from A_1 and A_2 as

the aggregated and single dansyl substituent states have different molar absorbances, ϵ , at 400 nm, the excitation wavelength, as indicated in Figure 1. As the absorbance data do not allow quantification of the dansyl substituent aggregation, as discussed above, A_1 and A_2 cannot be corrected for the differing aggregate and single dansyl ϵ values. The ϵ values of the βCD and $66\beta\text{CD}_2\text{ur}$ dansyl complexes are also different at 400 nm (see Supporting Information). The combination of these factors prevents the determination of apparent complexation constants from A_1 , A_2 , and A_3 .

Rheological Studies. The viscosity variation with shear rate of aqueous solutions 5 wt % in either PAADSen, PAADShn, or PAADSddn alone and in the presence of either βCD or $66\beta\text{CD}_2\text{ur}$ where the mole ratio of the dansyl substituents to either βCD or $66\beta\text{CD}_2\text{ur}$ is unity is shown in Figure 8. Therein the more viscous PAADSddn + $66\beta\text{CD}_2\text{ur}$ and PAADSddn solutions show small decreases in viscosity with increasing shear rate. The zero shear viscosity variations are shown in Figure 9. Three trends emerge, the first of which is that the PAADSddn solution is much more viscous than the PAADShn and PAADSen solutions consistent with the greater length of the dodecyl tether, allowing more aggregation between substituents on adjacent strands. A second trend is that the addition of βCD lowers the viscosity of all three solutions through complexation of the dansyl substituents and also their tethers in the case of PAADShn and PAADSddn and thereby decreases substituent aggregation. (A similar trend has been observed for octadecyl substituted poly(acrylate) where the high viscosity of its aqueous solution arising from substituent aggregation is greatly diminished by addition of βCD as a consequence of the octadecyl substituents being complexed by βCD .²⁵) In contrast, the addition of $66\beta\text{CD}_2\text{ur}$ increases the viscosity of all three solutions through host–guest complexation of dansyl substituents on adjacent strands to form interstrand linkages which are either stronger or more prevalent or both than dansyl substituent aggregation. These competing interactions are broadly shown for the PAADSddn system in Scheme 4.

CONCLUSIONS

Three new 3% randomly substituted poly(acrylate)s are reported in which the dansyl substituent tether lengthsens systematically as 2, 6, and 12 methylene groups are incorporated in PAADSen, PAADShn, and PAADSddn, respectively. For dilute aqueous solutions in which the interaction between substituted poly(acrylate) strands is minimal, UV–vis and time-resolved fluorescence studies are consistent with an equilibrium between aggregated and single dansyl substituents characterized by fluorescence lifetimes $\tau_1 = 2.2, 2.5,$ and 3.2 ns and $\tau_2 = 5.0, 5.3,$ and 9.5 ns, respectively, in the sequence PAADSen, PAADShn, and PAADSddn. Steady-state and time-resolved fluorescence and 2D ^1H NOESY NMR spectroscopy show the dansyl substituents to be complexed within the annulus of βCD in 1:1 host–guest complexes characterized by apparent complexation constants, $K = 89, 105,$ and 55 $\text{dm}^3 \text{mol}^{-1}$ and fluorescence lifetimes $\tau_3 = 13.2$ and 11.7 ns for the βCD .PAADSen and βCD .PAADShn complexes. However, τ_3 was not determined for βCD .PAADSddn because its signal amplitude was insufficient for accurate determination probably because a substantial proportion exists with βCD positioned over the dodecyl tether and has little effect on the dansyl substituent fluorescence. This also accounts for the smaller fluorescence change for PAADSddn on dansyl substituent

complexation by β CD than is the case for PAADSen and PAADShn. Cooperativity in dansyl substituent complexation by the two cyclodextrin annuli of 66β CD₂ur results in increases in 1:1 complex stability in the sequence $K = 3040, 34\,200$, and $242\,000\text{ dm}^3\text{ mol}^{-1}$ and $\tau_3 = 13.9, 20.8$, and 19.3 for the 66β CD₂ur.PAADSen, 66β CD₂ur.PAADShn, and 66β CD₂ur.PAADSddn complexes, respectively, coincident with the increasing dansyl substituent tether length decreasing poly(acrylate) backbone steric hindrance to complexation. These dilute solution observations aid the interpretation of rheological data for more concentrated solutions. Thus, the increase in zero shear viscosity in the sequence: PAADSen \sim PAADShn $<$ PAADSddn for aqueous solution indicates that dansyl substituent interstrand aggregation is favored with increase in substituent length, whereas dansyl substituent complexation by β CD decreases such aggregation. In contrast, viscosity increases in the sequence PAADSen \sim PAADShn $<$ PAADSddn in the presence of 66β CD₂ur as complexation of dansyl substituents from adjacent poly(acrylate) strands form interstrand linkages.

■ ASSOCIATED CONTENT

S Supporting Information. UV–vis temperature variations for substituted poly(acrylate)s, UV–vis variations for substituted poly(acrylate)s in the presence of β CD and 66β CD₂ur, steady-state and time-dependent fluorescence variations for the substituted poly(acrylate)s alone and in the presence of β CD and 66β CD₂ur, and 2D ^1H NOESY NMR spectra of the substituted poly(acrylate)s in the presence of β CD and 66β CD₂ur. This material is available free of charge via the Internet at <http://pubs.acs.org>.

■ AUTHOR INFORMATION

Corresponding Author

*E-mail: stephen.lincoln@adelaide.edu.au.

■ ACKNOWLEDGMENT

We gratefully acknowledge Australian Research Council funding, NSFC Grant 20774028 and 20774030, 111 Project Grant B08021, Shanghai Shuguang Plan Project 06SG35, Shanghai Pujiang Talent Project 07PJ14022, and the China Scholarship Council for supporting this work.

■ REFERENCES

- (1) Nabiokin, Y. V.; Ogurtsova, L. A.; Podgorny, V. P. *Opt. Spectrosc.* **1970**, *28*, 528.
- (2) Weber, W. H.; Lambe, J. *Appl. Opt.* **1976**, *5*, 229.
- (3) O'Connell, R. M.; Saito, T. T. *Opt. Eng.* **1983**, *4*, 393.
- (4) Arnold, M. A. *Anal. Chem.* **1992**, *64*, 1015A.
- (5) Barashkov, N. N.; Gunder, O. A. *Fluorescent Polymers*; Ellis Horwood: New York, 1994; p 152.
- (6) Premachandran, R. S.; Banerjee, S.; Wu, X.-K.; John, V. T.; McPherson, G. L. *Macromolecules* **1996**, *29*, 6460.
- (7) Anghel, D. F.; Alderson, V.; Winnik, F. M.; Mizusaki, M.; Morishima, Y. *Polymer* **1998**, *39*, 3035.
- (8) Hu, Y.; Armentrout, R. S.; McCormick, C. L. *Macromolecules* **1997**, *30*, 3538.
- (9) Schillén, K.; Anghel, D. F.; Miguel, M. d. G.; Lindman, B. *Langmuir* **2000**, *16*, 10528.
- (10) Hayashida, O.; Hamachi, I. *J. Org. Chem.* **2004**, *69*, 3509.
- (11) Prazeres, T. J. V.; Beingessner, R.; Duhamel, J. *Macromolecules* **2001**, *34*, 7876.
- (12) Kanagalingam, S.; Nagan, C. F.; Duhamel, J. *Macromolecules* **2002**, *35*, 8560.
- (13) Kanagalingam, S.; Spartalis, J.; Cao, T.-M.; Duhamel, J. *Macromolecules* **2002**, *35*, 8571.
- (14) Seixas de Melo, J.; Costa, T.; Miguel, M. D. G.; Lindman, B.; Schillén, K. *J. Phys. Chem. B* **2003**, *107*, 12605.
- (15) Shea, K. J.; Sasaki, D. Y.; Stoddard, G. J. *Macromolecules* **1989**, *22*, 1722.
- (16) Shea, K. J.; Stoddard, G. J.; Sasaki, D. Y. *Macromolecules* **1989**, *22*, 4303.
- (17) Shea, K. J.; Stoddard, G. J. *Macromolecules* **1991**, *24*, 1207.
- (18) Asano, M.; Winnik, F. M.; Yamashita, T.; Horie, K. *Macromolecules* **1995**, *28*, 5861.
- (19) Halder, S.; Raghuraman, H.; Chattopadhyay, A. *J. Phys. Chem. B* **2008**, *112*, 14075.
- (20) Guo, X.; Abdala, A. A.; May, B. L.; Lincoln, S. F.; Khan, S. A.; Prud'homme, R. K. *Macromolecules* **2005**, *38*, 3037.
- (21) Guo, X.; Abdala, A. A.; May, B. L.; Lincoln, S. F.; Khan, S. A.; Prud'homme, R. K. *Polymer* **2006**, *47*, 2976.
- (22) Guo, X.; Wang, J.; Li, L.; Pacheco, C. R.; Fu, L.; Prud'homme, R. K.; Lincoln, S. F. *Polym. Mater. Sci. Eng.* **2007**, *97*, 543.
- (23) Guo, X.; Li, L.; Fu, L.; Prud'homme, R. K.; Lincoln, S. F. *Polym. Prepr.* **2007**, *48*, 217.
- (24) Li, L.; Guo, X.; Wang, J.; Liu, P.; Prud'homme, R. K.; May, B. L.; Lincoln, S. F. *Macromolecules* **2008**, *41*, 8677.
- (25) Li, L.; Guo, X.; Fu, L.; Prud'homme, R. K.; Lincoln, S. F. *Langmuir* **2008**, *24*, 8290.
- (26) Kretschmann, O.; Choi, S. W.; Miyauchi, M.; Tomatsu, I.; Harada, A.; Ritter, H. *Angew. Chem., Int. Ed.* **2006**, *45*, 4361.
- (27) Harada, A.; Hashidzume, A.; Yamaguchi, H.; Takashima, Y. *Chem. Rev.* **2009**, *109*, 5974.
- (28) van de Manakkar, F.; Vermonden, T.; van Nostrum, C. F.; Hennink, W. E. *Biomacromolecules* **2009**, *10*, 3157.
- (29) Yhaya, F.; Gregory, A. M.; Stenzel, M. H. *Aust. J. Chem.* **2010**, *63*, 195.
- (30) Tamesue, S.; Takashima, Y.; Yamaguchi, H.; Shinkai, S.; Harada, A. *Angew. Chem., Int. Ed.* **2010**, *49*, 7461.
- (31) Yamaguchi, H.; Kobayashi, R.; Takashima, Y.; Hashidzume, A.; Harada, A. *Macromolecules* **2011**, *44*, 2395.
- (32) Harada, A.; Kobayashi, R.; Takashima, Y.; Hashidzume, A.; Hashidzume, A. *Nature Chem.* **2011**, *3*, 34.
- (33) Protonic Software, 2 Templegate Avenue, Leeds LS15 0HD, UK (www.hyperquad.co.uk).
- (34) SPC Image. Becker and Hickl, GmbH. Nahmitzer Damm 30, 12277 Berlin, Germany (www.becker-hickl.de/software/tcspc/software-etcspcspecial.htm).
- (35) Ultrafast Systems LLC, 1748 Independence Blvd. Suite G-6, Sarasota, FL 34234 (www.ultrafastsystems.com).
- (36) Chem3D Ultra, CambridgeSoft Co., 100 Cambridge Park Drive, Cambridge, MA 02140.
- (37) Ikeda, H.; Nakamura, M.; Ise, N.; Oguma, N.; Nakamura, A.; Ikeda, T.; Toda, F.; Ueno, A. *J. Am. Chem. Soc.* **1996**, *118*, 10980.
- (38) Ikeda, H.; Nakamura, M.; Ise, N.; Toda, F.; Ueno, A. *J. Org. Chem.* **1997**, *62*, 1411.
- (39) Ueno, A.; Ikeda, A.; Ikeda, H.; Ikeda, T.; Toda, F. *J. Org. Chem.* **1999**, *64*, 382.